Quantitative Analysis of Phosphotyrosine Signaling Networks Triggered by CD3 and CD28 Costimulation in Jurkat Cells[1]

Ji-Eun Kim and Forest M. White[2]

The mechanism by which stimulation of coreceptors such as CD28 contributes to full activation of TCR signaling pathways has been intensively studied, yet quantitative measurement of costimulation effects on functional TCR signaling networks has been lacking. In this study, phosphotyrosine networks triggered by CD3, CD28, or CD3 and CD28 costimulation were analyzed by site-specific quantitative phosphoproteomics, resulting in identification of 101 tyrosine and 3 threonine phosphorylation sites and quantification of 87 sites across four cell states. As expected, CD3 stimulation induced phosphorylation of CD3 chains and upstream components of TCR pathways such as Zap70, while CD28 stimulation induced phosphorylation of CD28, Vav-1, and other adaptor proteins including downstream of tyrosine kinase 1, Grb2-associated protein 2 (Grap2), and Wiskott-Aldrich syndrome protein. CD3 and CD28 costimulation induced a complex response including decreased threonine phosphorylation in the ERK1 and ERK2 activation loops and increased phosphorylation of selected tyrosine sites on ERK1/2, p38, phospholipase C-γ, Src homology 2 domain-containing transforming protein 1, Grap2, and Vav-1, potentiating T cell activation. Hierarchical clustering and self-organizing maps were used to identify modules of coregulated phosphorylation sites within the network. Quantitative information in our study suggests quantitative and qualitative contribution by costimulation of CD28 on CD3-stimulated TCR signaling networks via enhanced phosphorylation of phospholipase C-γ/Src homology 2 domain-containing transforming protein 1/Grap2/Vav-1 and their effects on downstream components including MAPKs. *The Journal of Immunology,* **2006, 176: 2833–2843.**

Studies on T cell activation leading to diverse cellular outcomes such as cytokine production have resulted in identification of a number of cellular components involved in T cell signaling pathways (reviewed in Refs. 1–4). Briefly, once the MHC molecule presents processed Ag to TCR α- and β-chains, CD4 binds to the MHC molecule, resulting in the proximity of lymphocyte-specific protein kinase (Lck),[3] which exists in a complex with CD4, to CD3-ζ and thereby phosphorylation of CD3 chains in the preexisting molecular cluster within plasma membrane microdomains. Each CD3 chain (CD3-δ, -ϵ, -γ) contains two phosphotyrosine sites in the ITAM motif (ITAM; YxxI/L) with the exception of the ζ-chain, which possesses six phosphotyrosine sites. TCR Zap70 is then recruited, binds to phosphorylated CD3 chains, and becomes phosphorylated by Lck. Phosphorylated Zap70, in turn, phosphorylates phospholipase C-γ (PLC-γ), which is promoted after its binding to an adaptor protein, linker for activation of T cells (LAT), and Src homology 2 domain-containing leukocyte protein of 76 kDa (SLP-76). PLC-γ can further activate protein kinase C (PKC), leading to NF-κB transactivation, and calcium-dependent pathways, resulting in the transport of NF-AT into the nucleus for its transcription activation. During early phosphorylation events in lipid raft clusters, Src homology 2 domain-containing transforming protein 1 (Shc) also interacts with phosphorylated ITAM in the ζ-chain and LAT, which interacts with other adaptor molecules such as Vav-1 or Ras via Grb2 and Grap2/Grb2-associated protein downstream of Shc (Gads), leading to the activation of MAPKs such as JNK, p38, and ERK 1/2 for subsequent AP-1 transactivation.

The two-signal theory suggests that T cell activation requires both Ag recognition via the TCR-CD3 complex and additional costimulatory signals derived from CD28 and other receptors (5). Correspondingly, CD28-negative mice require repeated stimulation to elicit T cell response and respond poorly to immunological challenge (reviewed in Ref. 6). Studies on the mechanism by which costimulation of CD3 and other coreceptors, particularly CD28, leads to complete activation of T cells have generated two hypotheses of T cell activation by CD3/CD28 costimulation, referred to as either the quantitative or qualitative mechanisms (6–8) The quantitative mechanism proposes *cis*-activation of the TCR signaling network by CD28 stimulation, affecting the phosphorylation level and activation of components downstream of the TCR to overcome a threshold necessary for T cell activation. Promotion of TCR localization with lipid rafts and reorganization of membrane microdomains have supported these quantitative effects of CD28 costimulation (6, 8–10). Additionally, the quantitative mechanism emphasizes the role of Vav-1 as an important effector in the CD28 signaling pathway and proposes that the activation of Vav-1 might differ from the CD3 signaling pathway, possibly through prolonged Lck activation (8). The qualitative mechanism

Biological Engineering Division, Massachusetts Institute of Technology, Cambridge, MA 02139

Received for publication September 26, 2005. Accepted for publication December 8, 2005.

The costs of publication of this article were defrayed in part by the payment of page charges. This article must therefore be hereby marked *advertisement* in accordance with 18 U.S.C. Section 1734 solely to indicate this fact.

[1] This work was supported by National Institutes of Health Grants R21-AI065354-2, P50-GM68762, R01-AI065824, and P30-ES002109.

[2] Address correspondence and reprint requests to Dr. Forest M. White, Biological Engineering Division, Massachusetts Institute of Technology, 77 Massachusetts Avenue, Room 56-787A, Cambridge, MA 02139. E-mail address: fwhite@mit.edu

[3] Abbreviations used in this paper: Lck, lymphocyte-specific protein kinase; IMAC, immobilized metal-affinity chromatography; MS, mass spectrometry; LC, liquid chromatography; PLC-γ, phospholipase C-γ; LAT, linker for activation of T cell; SLP-76, Src homology 2 domain-containing leukocyte protein of 76 kDa; PKC, protein kinase C; Grap2, Grb2-associated protein 2; Shc, Src homology 2 domain-containing transforming protein 1; Gads, Grb2-associated protein downstream of Shc; o.d., outside diameter; i.d., inside diameter; GEM, glycolipid-enriched membrane microdomain; WASP, Wiskott-Aldrich syndrome protein; SOM, self-organizing map; PAG, phosphoprotein associated with GEM; Gsk, glycogen synthase kinase 3; Itk, IL-2-inducible T cell kinase; SLAP-130, SLP-76-associated protein 130; Dok-1, downstream of tyrosine kinase 1.

0022-1767/06/$02.00

focuses more on *trans*-activation of the TCR signaling network, with CD28 stimulation resulting in distinct signaling pathways leading to cytoskeleton rearrangement and mediation by key proteins such as PI3K, Vav-1, and SLP-76 (7). In fact, cytoskeletal scaffolding following T cell stimulation is indispensable for T cell activation (11).

Studies to elucidate signaling pathways triggered by TCR stimulation or TCR and coreceptor stimulation have identified many of the components, their interactions, and protein phosphorylation sites in the TCR signaling network under a variety of conditions. These efforts have generated a fairly comprehensive map of the T cell signaling pathways, but quantitative functional analysis of T cell signaling components regulating responses to costimulation at the network level has been lacking. To elucidate the molecular mechanism of CD3/CD28 costimulation, a site-specific quantitative analysis of phosphotyrosine protein networks in CD-3, CD28-, and CD3/CD28-costimulated Jurkat cells was performed using a recently developed mass spectrometry (MS)-based phosphoproteomics method (12). Data analyzed in this study provide quantitative information on the role of both specific protein phosphorylation sites and functional modules effecting T cell activation following CD3 and CD28 costimulation.

Materials and Methods

Cell culture and TCR stimulation

Human Jurkat T cell line (provided by the Lauffenburger Laboratory in the Massachusetts Institute of Technology Biological Engineering Division) was maintained in RPMI 1640 (Invitrogen Life Technologies) supplemented with 10% heat-inactivated FBS, 2 mM L-glutamine, 0.1 mM nonessential amino acid solution, 10 mM HEPES buffer, 100 U/ml penicillin, 100 μg of streptomycin, 1 mM sodium pyruvate, and 55 μM 2-ME (Invitrogen Life Technologies) at 37°C under 5% CO_2. Cells were grown in 75-cm^3 flasks with a starting density of 3×10^5/ml for 48 h, serum-starved for 12 h, and divided into phosphate buffer saline (PBS) with a density of 2×10^7/ml followed by incubation for 5 min at 37°C. Cells were treated for 5 min at 37°C with 2 μg/ml isotype control Ab (Pierce), 2 μg/ml mouse IgG anti-human CD3 Ab (clone HIT3a; BD Biosciences), mouse IgG anti-human CD28 Ab (clone CD28.2; BD Biosciences), or 2 μg/ml mouse IgG anti-human CD3 Ab and mouse IgG anti-human CD28 Ab with goat anti-mouse IgG Ab (Pierce,) for cross-linking. The reaction was stopped by cold PBS followed by centrifugation for subsequent lysis.

Cell lysis, protein reduction, alkylation, and digestion

Cells were lysed with 8 M urea supplemented with 1 mM sodium orthovanadate (Sigma-Aldrich) and incubated for 20 min on ice. Fifty-microliter aliquots were used to measure protein concentration with the bicinchoninic acid assay (Pierce) according to the manufacturer's instruction. Cell lysates were reduced with 10 mM DTT for 1 h at 56°C followed by alkylation with 55 mM iodoacetamide for 1 h. Cell lysates were diluted (five times) with 100 mM ammonium acetate (pH 8.9) and digested with 60 μg of trypsin (Promega) overnight at room temperature. Digested cell lysates were desalted using Sep-Pak (Millipore) and lyophilized as described previously (12).

iTRAQ modification and peptide immunoprecipitation

Peptides were labeled with iTRAQ reagents (Applied Biosystems) according to the manufacturer's instruction. Briefly, lyophilized peptides derived from 1×10^7 cells (200 μg of protein) were dissolved in 0.5 M triethylammonium bicarbonate and reacted for 1 h with two tubes of the iTRAQ reagents dissolved in ethanol (e.g., 200 μg of peptide from control sample was reacted with 2 tubes of iTRAQ-114). After incubation, samples labeled with four different iTRAQ reagents were combined and concentrated for subsequent immunoprecipitation with an anti-phosphotyrosine Ab mixture (12 μg each of pTyr100 from Cell Signaling Technology and PT66 from Sigma-Aldrich) bound to protein G-linked agarose beads in immunoprecipitation buffer (30 mM Tris, 30 mM NaCl, and 0.3% Nonidet P-40, pH 7.4) overnight at 4°C. The beads were washed with rinse buffer (100 mM Tris, 100 mM NaCl, and 0.3% Nonidet P-40, pH 7.4) three times and twice with immunoprecipitation buffer without Nonidet P-40. After the final rinse, immunoprecipitated peptides were eluted with 100 mM glycine (pH 2.5) for further immobilized metal affinity chromatography (IMAC)-based phosphopeptide enrichment.

Phosphopeptide enrichment using IMAC

IMAC columns were prepared as described elsewhere (13). Briefly, a 15-cm long (360 μm outside diameter (o.d.) $\times$ 200 μm inside diameter (i.d.)) microcapillary fused-silica column (Polymicro Technologies) was packed with POROS 20MC in water (Applied Biosystems) and washed with 100 mM EDTA (10 min at 10 μl/min). After rinsing with water to remove EDTA, the column was charged with 100 mM $FeCl_3$ for 10 min at 10 μl/min. Excess $FeCl_3$ was removed by rinsing with 0.1 M acetic acid, and the column was equilibrated with 0.1% trifluoroacetic acid. Immunoprecipitated peptides in 30% acetonitrile and 0.1% trifluoroacetic acid were loaded into the IMAC column at 1 μl/min. Remaining nonphosphorylated peptides were removed by washing with organic buffer comprised of 30% acetonitrile and 0.1% trifluoroacetic acid. The column was then equilibrated with 0.1% acetic acid (10 min at 10 μl/min) and phosphopeptides were eluted with 250 mM NaH_2PO_4 (pH 8.0) into a 10-cm long (360 μm o.d. $\times$ 100 μm i.d.) microcapillary fused silica precolumn packed with 10 μm C18 (YMC).

Liquid chromatography and tandem MS

After rinsing to remove excess phosphate buffer, the precolumn was connected to a 10-cm long (360 μm o.d. $\times$ 50 μm i.d.) microcapillary fused silica analytical column (packed with 5 μm C18 (YMC ODS-AQ)) with an integrated electrospray ionization tip ($\sim$1 μm). Peptides were eluted using a 120-min gradient: 0–13% B in 10 min, 13–42% B in 95 min, 42–60% B in 10 min, and 60–100% B in 5 min (B = 70% acetonitrile, 0.2 M acetic acid) and electrosprayed directly into a quadruple-time-of-flight mass spectrometer (QSTAR XL Pro; Applied Biosystems) with a flow rate $<$50 nl/min. The instrument was run in positive ion mode and cycled through information-dependent acquisition of a full-scan mass spectrum (*m/z*, 400-1500) (1.5 s), followed by four MS/MS scans (3 s each) sequentially on the four most abundant ions with two to five charges present in the full-scan mass spectrum.

Data analysis

All MS/MS spectra were searched against a human protein database (National Center for Biotechnology Information) with both MASCOT (Matrix Science) and ProQuant (Applied Biosystems) database searching algorithms. Search parameters contained a variable modification of +80 Da on serine, threonine, and tyrosine; variable neutral loss from phosphorylated serine and threonine amino acids, fixed modifications of carbamoyl at cysteine, and iTRAQ at amino-terminal and lysine. Example spectra and process for sequence identification and quantification are shown in Fig. 1*B*. The majority of the fragment ions were automatically assigned to y- or b-type fragment ions in phosphorylated peptides. Phosphorylation sites and peptide sequence assignments contained in MASCOT or ProQuant search results were validated by manual confirmation from raw MS/MS data. Peak areas for each of four signature peaks (*m/z*: 114, 115, 116, 117, respectively) were obtained from ProQuant and corrected for isotopic overlap.

Bioinformatics and statistical analysis

Peak areas were normalized with values from the peak areas of nonphosphorylated peptides in supernatant of immunoprecipitation (analyzed separately by liquid chromatography (LC)-MS/MS). Each treatment was normalized against control sample to obtain an induced level of phosphorylation in CD3, CD28, and CD3/CD28 costimulation. Final normalized data sets (in Excel spreadsheets) were loaded into Spotfire and self-organizing maps and hierarchical analysis from Spotfire were used to cluster phosphorylation sites using built-in functions of the program. All of the statistical *p* value was obtained from the one-tailed Student *t* test performed in Excel.

Western blotting

Cell lysates were prepared by three freeze-thaw cycles in lysis buffer (20 mmol/L Tris-HCl, 150 mmol/L NaCl, 1 mmol/L EDTA, 1% Triton X-100, 0.5% Igepal, 2.5 mmol/L sodium PP_i, 1 mmol/L β-glycerophosphate, 1 mmol/L sodium orthovanadate, 1 μmol/L okadaic acid, 1 μg/ml leupeptin, 1 μg/ml bestatin, and 1 mmol/L phenylmethylsulfonyl fluoride) followed by centrifugation at 14,000 $\times$ *g* for 30 min. 7Seventy-five micrograms of total protein measured by the bicinchoninic acid protein assay (Pierce) was separated in 15% Tris-HCl gel (Bio-Rad) by SDS-PAGE and transferred onto a polyvinylidene difluoride membrane. The membrane was blocked with 5% nonfat milk in TBS with 0.1% Tween 20 for 1 h and then incubated with the indicated primary Ab in the same blocking buffer at 4°C

overnight. Rabbit anti-phospho Zap70 (Tyr^{292}) Ab, mouse anti-phospho ERK (Tyr^{204}) Ab (Santa Cruz Biotechnology), and mouse anti-phospho p44/42 MAPK (Thr^{202}/Tyr^{204}) Ab (Cell Signaling Technology) were used as primary Abs (1/1000 dilution). After washing with TBS and 0.1% Tween 20, the membrane was incubated with secondary anti-IgG Ab conjugated with HRP (1/100,000 dilution; Pierce) for 1 h. Blots were developed with supersignal West Femto substrate (Pierce). The membrane was reprobed with goat anti-actin Ab (Calbiochem) for normalization.

Results

Quantitative phosphoproteomics analysis of tyrosine phosphorylation in CD3-, CD28-, and CD3/CD28-costimulated Jurkat T cells resulted in the identification of 101 tyrosine and 3 threonine phosphorylation sites from 76 proteins, 87 of which were quantified across four cell states (full data set available at http://web.mit.edu/fwhitelab/data). Briefly, protein extracts from stimulated Jurkat cells were enzymatically digested to peptides, which were chemically tagged before mixing. Tyrosine-phosphorylated peptides were isolated from the peptide mixture of four different cell states by immunoprecipitation, enriched by IMAC, and subjected to LC-MS/MS analysis (schematically represented in Fig. 1*A*). Following automated sequence assignment and quantification, manual validation was performed to eliminate quantification errors and to ensure accuracy of sequence and phosphorylation site assignment using raw data (an example is shown in Fig. 1*B*). Relative peak areas from iTRAQ marker ions (highlighted *bottom left* in Fig. 1*B*) present in the MS/MS analysis are representative of the level of phosphorylation on the given peptide from each of the four samples used for quantification.

Regulation of tyrosine phosphorylation in CD3 ITAMs and upstream kinases

ITAMs in CD3 and most of the upstream kinases identified in the data responded to CD3 stimulation but did not appear to play a role in the CD3/CD28 costimulation mechanism (other than PLC-γ). Tyrosine phosphorylation levels were quantified for every known ITAM of CD3δ, ϵ, γ, and ζ (Fig. 2*A*). Phosphorylation levels for each ITAM tyrosine site were increased 2- to 4-fold by CD3 stimulation, but were not further affected by CD3/CD28 costimulation (Fig. 2, *B* and *C*). Among protein kinases interacting with CD3 chains, phosphorylation sites in Lck and TCR Zap70) were identified and quantified (Fig. 3, *B* and *C*). Three tyrosine phosphorylation sites (Tyr^{192}, Tyr^{394}, and Tyr^{505}) on Lck were identified and quantified. Of these, the tryptic peptide containing Tyr^{394} (LIEDNEpYTAR) of Lck was quantified but could not be definitively assigned to Lck, Src, or Fyn because the peptide sequence is identical among these Src kinase family members. Phosphorylation of Tyr^{394} appeared to be constitutive and did not change in response to any of the stimulations. Phosphorylation of Tyr^{505} was up-regulated 3-fold by CD3 stimulation, was unaffected by CD28 stimulation, and was down-regulated by CD3/CD28 costimulation. For Zap70, CD3 stimulation increased phosphorylation at Tyr^{292}, a primary in vitro autophosphorylation site (14). Phosphorylation of this site was not further affected by CD3/CD28 costimulation (Fig. 3, *B* and *C*). In combination with phosphorylation of other downstream proteins, it seems that phosphorylation at Tyr^{292} in Zap70 corresponded with activation of the TCR pathway in this system, although it has been previously implicated in negative regulation using a mutated construct (15). Hierarchical clustering and self-organizing maps clustered Zap70 Tyr^{292} with CD3 ITAMs and PLC-γ (Fig. 4, *A* and *B*). Correspondingly, Zap70 has been implicated in transducing early T cell activation signaling from CD3 chains to downstream proteins such as PLC-γ (1–4). Finally, to compare with the quantitative MS data, Western blots were performed with an Ab recognizing Zap70 phosphorylated at Tyr^{292}. Tyrosine phosphorylation levels measured by these two disparate analysis methods are in close agreement, as demonstrated in Fig. 3*D*.

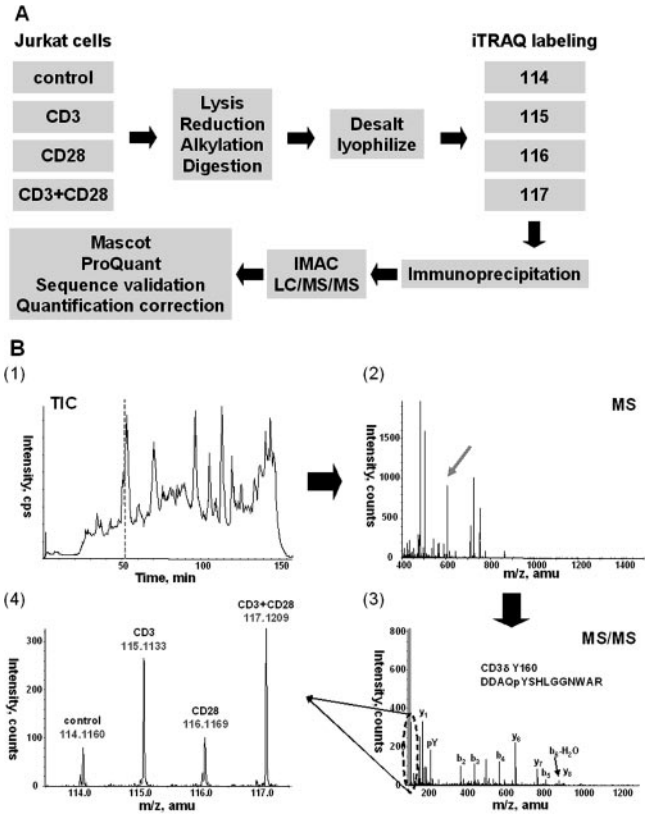

FIGURE 1. Experimental scheme. *A,* Experimental procedure. Briefly, Jurkat cells were serum starved (12 h) and stimulated (5 min) with either isotype control Ab, anti-human CD3 Ab, anti-human CD28 Ab, or anti-human CD3 Ab and anti-human CD28 Ab with goat anti-mouse IgG Ab for cross-linking. Following stimulation, cells were lysed, proteins were denatured and enzymatically digested to peptides, and peptides were chemically tagged before mixing. Tyrosine-phosphorylated peptides were isolated by immunoprecipitation with a mixture of anti-phosphotyrosine Abs, enriched by IMAC, and subjected to LC-MS/MS analysis. *B,* LC/tandem MS analysis and quantitative information from tandem MS spectrum. During LC-MS/MS analysis, peptides were acquired for ~2.5 h, during which time the instrument gathered >1000 MS spectra, each of which was queried to determine the four most abundant species, which were subsequently subjected to MS/MS analysis. Relative peak areas from iTRAQ marker ions present in the MS/MS analysis were quantified, representing the level of phosphorylation on the given peptide from each of the four samples. A peptide from CD3δ is presented as an example here: 1) TIC, Total ion chromatogram of peptide separation using LC; 2) MS, mass spectrum of selected time point; 3) MS/MS, tandem mass spectrum of selected peptide in a mass spectrum containing both sequence and quantification information (highlighted); and 4) signature peptide ions representing quantitative information in the low-mass range of tandem MS spectrum in *B* (graph 3). Each peak area is representative of the phosphorylation level of a tyrosine site in a peptide (DDAQpYSHLGGNWAR; CD3δ Y160) from control (m/z = 114), CD3 stimulated (m/z = 115), CD28 stimulated (m/z = 116), and both CD3/CD28 costimulated (m/z = 117).

Tyrosine phosphorylation sites in PLC-γ and two downstream proteins, protein kinase C-δ (PKC-δ) and calmodulin, were also quantified in this study (Fig. 3, *B* and *C*). Within PLC-γ, both Tyr^{771} and Tyr^{775} were detected and quantified; sequence information from a tandem MS experiment was sufficient to distinguish the peptides phosphorylated at two different tyrosine residues despite their proximity in the same peptide. Although both phosphorylation sites showed a similar level of increase in response to CD3

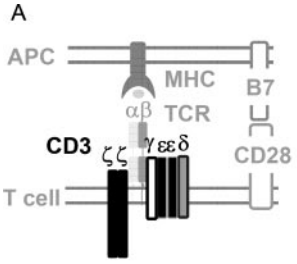

B

CD3 chain	Phosphosite	Ratio average ± standard deviation		
		CD3/Ctrl	CD28/Ctrl	CD3+CD28/Ctrl
CD3δ	Y149*	3.396±0.577	1.082±0.049	3.322±0.426
	Y160*	3.644±0.149	1.111±0.096	3.369±0.314
CD3ε	Y188*	3.483±0.148	1.057±0.091	2.896±0.299
	Y199*	3.074±0.156	1.115±0.062	3.229±0.080
CD3γ	Y160*	2.667±0.096	1.113±0.088	2.450±0.229
	Y171*	3.486±0.213	1.123±0.101	3.503±0.056
CD3ζ	Y72*	3.004±0.046	1.136±0.017	2.789±0.026
	Y83*	3.307±0.217	1.189±0.224	3.808±0.431
	Y111*	2.336±0.080	1.057±0.062	2.347±0.125
	Y123*	2.193±0.297	0.907±0.088	2.006±0.262
	Y142*	2.151±0.068	1.060±0.030	2.447±0.165
	Y153*	2.574±0.335	1.070±0.040	2.683±0.433

C

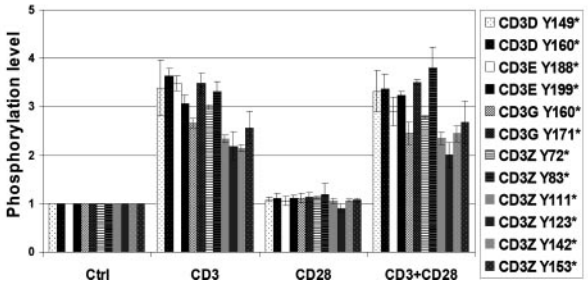

FIGURE 2. Regulation of phosphorylation sites in CD3 chains in response to T cell stimulation. *A,* CD3 chains in TCR. CD3-γ, -ϵ, and -δ chains have one ITAM containing two phosphotyrosine sites, whereas CD3ζ has three ITAMs and therefore six phosphotyrosine sites. *B,* Quantification results for specific tyrosine phosphorylation sites in CD3 chains in response to CD3, CD28, and CD3/CD28 costimulation. Data represent mean of results obtained from three experiments; ∗, Previously reported phosphorylation site. *C,* Changes in phosphorylation levels of specific phosphorylation sites in CD3 chains in responses to CD3, CD28, and CD3/CD28 costimulation. Ctrl, Control.

stimulation (Fig. 3, *B* and *C*), phosphorylation of Tyr^{775} was further increased by costimulation (Table I). Studies on PKC-δ have focused on its phosphorylation at serine/threonine residues (16), its proapoptotic function (17), and antiapoptotic role (18) in diverse systems. CD3 stimulation induced a 2.5-fold increase in phosphorylation of PKC-δ Tyr^{313}, a level of which was not further affected by CD3/CD28 costimulation (Fig. 3, *B* and *C*). The role of PKC-δ, and particularly phosphorylation at Tyr^{313} in the unique sequence compared with other PKCs (RSDSASSEPVGIpYQGFEK), has not been studied in T cell signaling. Both hierarchical clustering and self-organizing maps showed close connection of this site to CD3 chains, Shc, and p38 (Fig. 4, *A* and *B*). Relevantly, PKC-δ was reported to affect p38 MAPK in the IFN-α pathway in different cell lines (19). Phosphorylation of calmodulin in the Ca^{2+}-dependent pathway was also monitored; CD3 stimulation induced a 1.6-fold increase in phosphorylation at Tyr^{99} while CD3/CD28 costimulation did not further affect the phosphorylation level at this site (Fig. 3, *B* and *C*).

Regulation of tyrosine phosphorylation in adaptor proteins

Molecular adaptor/scaffold proteins play important roles by linking upstream kinases to downstream kinases or substrates (3, 20). LAT, Lck, and other adaptor proteins and kinases reside in glycolipid-enriched membrane microdomains/lipid rafts (GEM) under normal conditions. As shown schematically in Fig. 5*A*, other kinases and adaptor proteins are recruited to the GEM in response to TCR stimulation. Not surprisingly, quantitative changes in the phosphorylation level of many of the adaptor proteins were observed in response to CD3, CD28, or CD3/CD28 costimulation (Fig. 5, *B* and *C* (transmembrane adaptor proteins) and *D* (cytosolic adaptor proteins)). The most noticeable regulation is that CD3 stimulation increased phosphorylation of Tyr^{45} in Grb2-related adaptor protein 2 (Grap2, also known as Grb2-associated protein downstream of Shc (Gads)) by 2.4-fold and Tyr^{317} in Src homology 2 domain-containing transforming protein 1 (Shc) by 2.3-fold while CD3/CD28 costimulation further amplified their phosphorylation by 59 and 24%, respectively, suggesting their regulatory roles in response to CD3/CD28 costimulation (Table I). Grap2 shows similar SH3 binding specificity to Grb-2, but is expressed specifically in hemopoietic cells and known to interact with LAT, Sos, dynamin, sam68, and SLP-76, leading to Ag-stimulated endocytosis of TCR, cell proliferation, and cell cycling (3, 20). In both self-organizing maps and hierarchical clustering, Grap2 was clustered with CD3 chains, Zap70, and PLC-γ (Fig. 4,

A

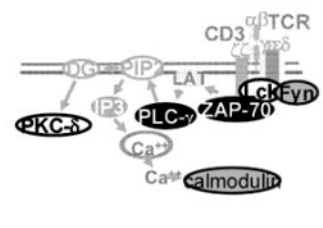

B

Protein	Phosphosite	Ratio average ± standard deviation		
		CD3/Ctrl	CD28/Ctrl	CD3+CD28/Ctrl
Lck	Y191*	1.046±0.021	0.989±0.018	0.892±0.036
	Y393*	1.154±0.055	1.017±0.025	0.998±0.003
	Y504*	2.951	1.041	0.883
ZAP-70	Y292*	3.530±0.236	1.145±0.046	3.052±0.354
PLC-γ	Y771*	2.925±0.113	1.052±0.039	3.001±0.777
	Y775*	2.868±0.498	1.126±0.031	3.612±0.628
PKC-δ	Y313*	2.516±0.231	1.275±0.095	2.422±0.046
calmodulin	Y99*	1.615±0.209	1.087±0.067	1.595±0.182

C

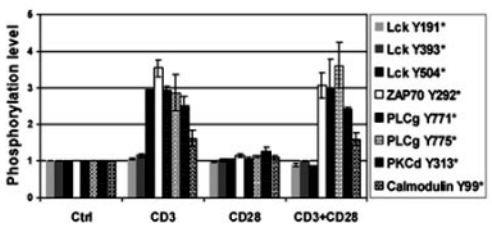

D

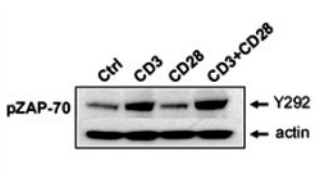

FIGURE 3. Regulation of phosphorylation sites in protein tyrosine kinases and key components in the PLC-γ pathway in response to T cell stimulation. *A,* Protein tyrosine kinases interacting with CD3 chains and components in the PLC-γ pathway. *B,* Quantification results for specific tyrosine phosphorylation sites in protein tyrosine kinases in response to CD3, CD28, and CD3/CD28 costimulation. Data represent mean of results obtained from three experiments; ∗, Previously reported phosphorylation site. Phosphorylation at Tyr^{504} in Lck was detected in one analysis, but with multiple independent MS/MS scans. *C,* Changes in phosphorylation level of specific phosphorylation sites in Zap70, Lck, PLC-γ, PKC-δ, and calmodulin in response to CD3, CD28, and CD3/CD28 costimulation. *D,* Western blotting for a specific tyrosine phosphorylation site in Zap70. Data are representative of three experiments. Actin was used as a loading control (Ctrl).

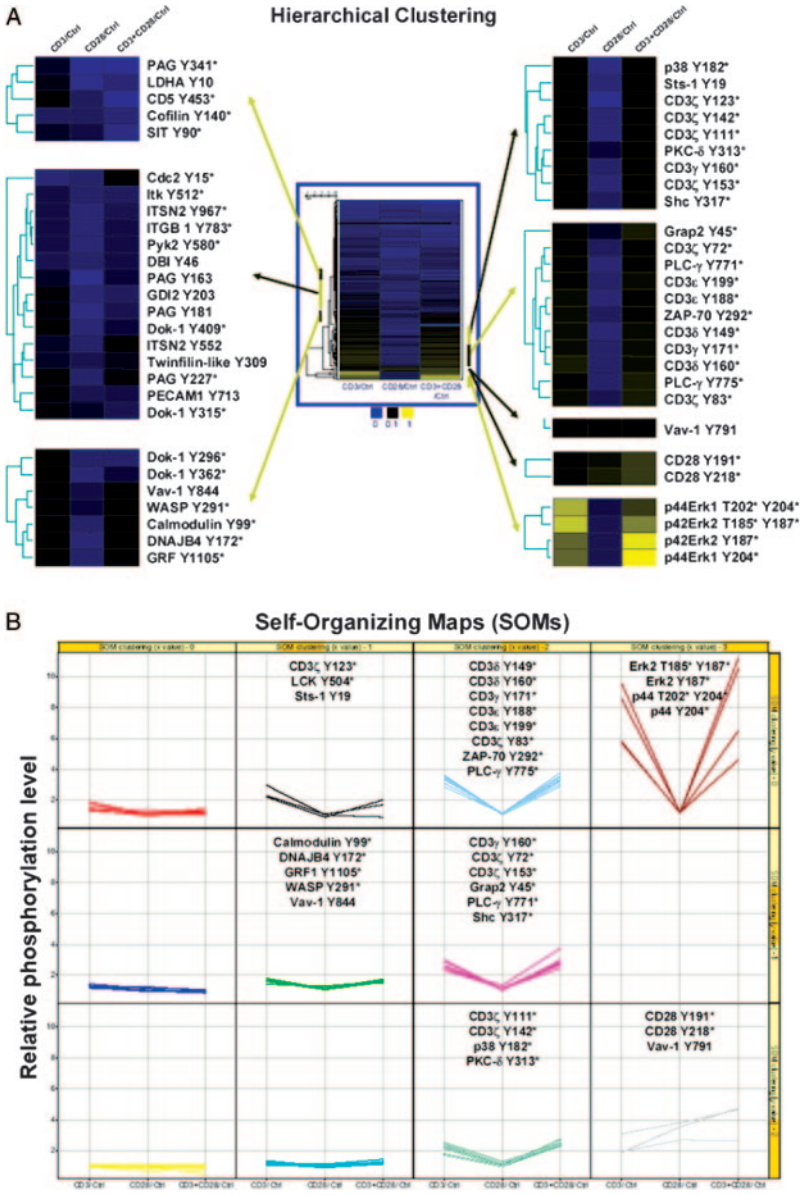

FIGURE 4. Clustering analysis of phosphotyrosine protein networks in stimulated Jurkat cells. *A,* Hierarchical clustering analysis. Three columns represent relative phosphorylation level in CD3-, CD28-, and CD3/CD28-costimulated Jurkat cells normalized against that in control cells. Yellow represents highly induced phosphorylation level and blue represents control level phosphorylation. Selected examples of clustered phosphorylation sites are highlighted. *B,* Clustering analysis using SOMs. Three columns represent the relative phosphorylation level in CD3-, CD28-, and CD3/CD28-costimulated Jurkat cells normalized against that in control cells. Optimal SOM architecture was a 3×4 matrix, as smaller matrices tended to cluster obviously dissimilar phosphorylation profiles.

A and *B*). These data, along with the highly amplified phosphorylation level in costimulation, suggest that Grap2 is regulated along with other upstream kinases during response to CD3 stimulation and moreover may be a critical regulator in CD3/CD28 costimulation. It is interesting to note that phosphorylation of Shc Tyr^{317} has been implicated in regulating the specific interaction between Shc and Grap2 (21), which may explain the coregulation of these proteins in our study. Tyr^{317} of p52 Shc was reported to be preferred by Lck whereas other sites such as Tyr^{239} and Tyr^{240} were phosphorylated by Syk and Zap70 in an overexpressed cell line system (22). However, our data showed better correlation between Tyr^{317} of Shc and Zap70 as compared with Lck (Figs. 3*B* and 6*B*). In hierarchical clustering and self-organizing maps, Shc Tyr^{317} phosphorylation was clustered closely with CD3-ζ Tyr^{111}, Tyr^{142}, and Tyr^{153} and CD3-γ Tyr^{160} (also along with PKC-δ, p38, and Vav-1) (Fig. 4, *A* and *B*). In agreement with these results, Ravichandran et al.(23) have reported Shc binding to the phosphorylated CD3-ζ chain.

Vav-1 has been highlighted in CD28 signaling and in response to CD3/CD28 costimulation (7, 8). Phosphorylation of Vav-1 was increased in response to both CD3 and CD28 stimulation by 1.9- and 2.7-fold for Tyr^{791} and 1.45- and 1.25-fold for Tyr^{844}, respectively (Fig. 5, *B* and *D*). CD3/CD28 costimulation increased CD3-induced phosphorylation at Tyr^{791} by 38%, implying its involvement in costimulation (Table I). Phosphorylation at Tyr^{291} in the Wiskott-Aldrich syndrome protein (WASP) has been implicated in actin polymerization (24) and binding to Cdc42 (25). In our data set, WASP Tyr^{291} showed a pattern similar to Vav-1 Tyr^{844} (Fig. 5, *B* and *D*) with a slight increase (11%) in CD3/CD28 costimulation (Table I). WASP is also known to interact with intersectin-2 (26), an adaptor molecule involved in clathrin-coated vesicles and thereby in TCR endocytosis, which occurs a few minutes after TCR stimulation only if CD3 is fully activated (1). Hierarchical clustering shows a high correlation between tyrosine phosphorylation sites on WASP and Vav-1, which was also known to be involved in actin filamentation (7) (Fig. 4*A*). Self-organizing maps also cluster WASP Tyr^{291} with Vav-1 Tyr^{844} and calmodulin Tyr^{99} (Fig. 4*B*).

For the other members of the group of adaptor proteins, only minimal changes were seen for phosphorylation levels of SLP-76 associated protein (SLAP-130; also called Fyn-binding protein (Fyb-120/130)) and Src family-associated phosphoprotein 1 (Fig.

Table I. *Quantitative effects of CD3 and CD28 costimulation on CD3-stimulated phosphorylation*

Protein	Phosphosite	Increase or Decrease by Costimulation (%)
CD28	Y191*	150.7
p44Erk1	Y204*	97.6
P42Erk2	Y187*	84.6
Grap2/Gads	Y45	59.0
p38	Y182*	56.9
CD28	Y218	50.4
Vav-1	Y791	37.9
Cdc2	Y15*	33.8
PLC-γ	Y775*	25.9
Shc	Y317*	24.1
Ribosomal protein P0	Y24	18.2
CD3ζ	Y83*	15.2
Activating NKR	Y308	13.9
CD3ζ	Y142*	13.8
Talin 1	Y70	12.5
WASP	Y291*	11.2
ITSN2	Y552	10.7
Amylo-1,6-glucosidase	Y584	−10.4
PECAM1	Y713	−11.0
Lck	Y393*	−13.5
Zap70	Y292*	−13.5
Dok-1	Y409*	−14.7
Lck	Y191*	−14.7
PAG	Y181	−14.8
TK2	Y292*	−15.1
Protein tyrosine phosphatase, receptor type, A	Y798*	−15.4
PI-3K	Y467	−15.6
Dok-1	Y315*	−16.1
CD3ε	Y188*	−16.8
PAG	Y417*	−18.5
Eukaryotic translation elongation factor 1α	Y85	−19.1
GDP dissociation inhibitor 2 (GDI-2)	Y203	−19.2
PAG	Y387	−21.8
Lactate dehydrogenase A	Y10	−21.9
SHP2-interacting transmembrane adaptor protein	Y90*	−23.0
Sts-1	Y19	−25.4
PAG	Y341*	−31.9
p42ERk2	T185* Y187*	−32.0
Dok-1	Y362*	−32.6
Dok-1	Y296*	−36.4
CD5	Y453*	−39.3
Cdc2	T14* Y15*	−43.5
p44Erk1	T202* Y204*	−45.7
Lck	Y504*	−70.1

*, Previously reported phosphorylation site.

5, *B* and *D*). Both downstream of tyrosine kinase 1 (Dok-1) and phosphoprotein associated with glycosphingolipid-enriched microdomains (PAG) were constitutively phosphorylated as previously reported (27, 28). Phosphorylation levels at multiple sites in Dok-1 and PAG were increased slightly following CD3 stimulation; this effect was largely abolished by CD3/CD28 costimulation (Fig. 5, *B–D*), similar to the pattern displayed by Lck Tyr^{505}.

Regulation of phosphorylation in MAPKs

ERK2 (p42) and ERK1 (p44) are MAPKs activated downstream of Ras (Fig. 6*A*). Although the level of the doubly phosphorylated (active) form of p42 and p44 increased dramatically (by 9.5- and 8.5-fold, respectively) in response to CD3 stimulation, this level decreased significantly (by 32 and 45.7%, respectively) in response to CD3/CD28 costimulation (Fig. 6, *B* and *C*). By comparison, the singly phosphorylated form of these proteins increased 5.8- and 5.7-fold, respectively, in response to CD3 stimulation (Fig. 6, *B* and *C*), whereas CD3/CD28 costimulation further amplified this response by 81.6 and 97.6%, respectively (Table I). In contrast to our MS data, Western blotting using an Ab recognizing the doubly phosphorylated form of p42/44 shows an apparent increase following CD3/CD28 costimulation, a pattern of which was also seen when Western blots were probed with an Ab recognizing the singly phosphorylated form of these proteins (Fig. 6*D*). Based on the similarity between these Western blots, it is likely that the specificity of these Abs is insufficient to correctly quantify the relative phosphorylation levels of the two isoforms of these proteins. It is worth noting that the sequences of p42 and p44, while homologous, are divergent enough to readily distinguish each protein (and each phospho-isoform) by MS (Fig. 6*E*). Quantitative analysis of singly phosphorylated p38 shows a similar pattern to singly phosphorylated p42/p44, albeit with a lower increase in absolute magnitude as compared to the other two MAPKs and no doubly phosphorylated form was detected (Fig. 6, *B* and *C*).

Regulation of tyrosine phosphorylation in components of CD28 signaling pathways

Whether CD28 contributes to TCR signaling pathways qualitatively or quantitatively remains a question in T cell activation. Identification of components regulated distinctively in response to CD28 stimulation was therefore of interest in this study. Several CD28 tyrosine phosphorylation sites have been described in the literature. Tyr^{191} in the YMNM motif of the CD28 cytoplasmic tail (7, 8) has been shown to recruit PI3K and negatively regulate HIV-1 transcription (29). Tyr^{218} in CD28 was also shown to be involved in Vav-1 tyrosine phosphorylation, Rac1 activity (30) and, along with Tyr^{206} and Tyr^{209}, in IL-2 secretion (31). Not surprisingly, both CD28 stimulation and CD3/CD28 costimulation resulted in increased phosphorylation levels of CD28 Tyr^{191} and Tyr^{218}. Interestingly, in our data set, phosphorylation levels of CD28 Tyr^{191} and Tyr^{218} were increased by CD3 stimulation (Fig. 7, *B* and *C*), which suggests recruitment of CD28 into lipid rafts, potentially resulting in its phosphorylation by shared protein tyrosine kinases activated during CD3 stimulation. The phosphorylation level of PI3K p85 Tyr^{467} and glycogen synthase kinase 3β (Gsk3) Tyr^{279} were unaffected by CD3, CD28, or CD3/CD28 costimulation. However, CD3 stimulation induced a 23% increase ($p < 0.001$) in phosphorylation at Tyr^{512} of IL-2-inducible T cell kinase (Itk). Phosphorylation of this site has previously been linked to Lck activity and is reported to activate Itk (32) (Fig. 7, *B* and *C*). In Jurkat cells, PI3K and Itk are known to be constitutively active due to the high level of phosphatidylinositol(3,4,5)triphosphate from phosphatase and tension analog deficiency (33–35).

Clustering of identified phosphorylation sites in CD3, CD28, and CD3/CD28 costimulation

To identify coregulated phosphorylation sites, the data were clustered using both hierarchical clustering (Fig. 4*A*) and self-organizing maps (Fig. 4*B*). In hierarchical clustering, sites most closely coregulated are grouped together and a distance metric is provided to estimate the variance between clusters of grouped sites. This method was able to successfully cluster phosphorylation sites expected to be coregulated such as the singly and doubly phosphorylated forms of ERK1 and ERK2. A different cluster contained many of the phosphorylation sites on CD3 chains along with sites on Grap2, PLC-γ, and Zap70, while a closely related cluster contained the remainder of the CD3 tyrosine phosphorylation sites, p38, Sts-1, PKC-δ, and Shc (Fig. 4*A*). Self-organizing maps (SOMs) have been applied to cluster self-similar temporal gene

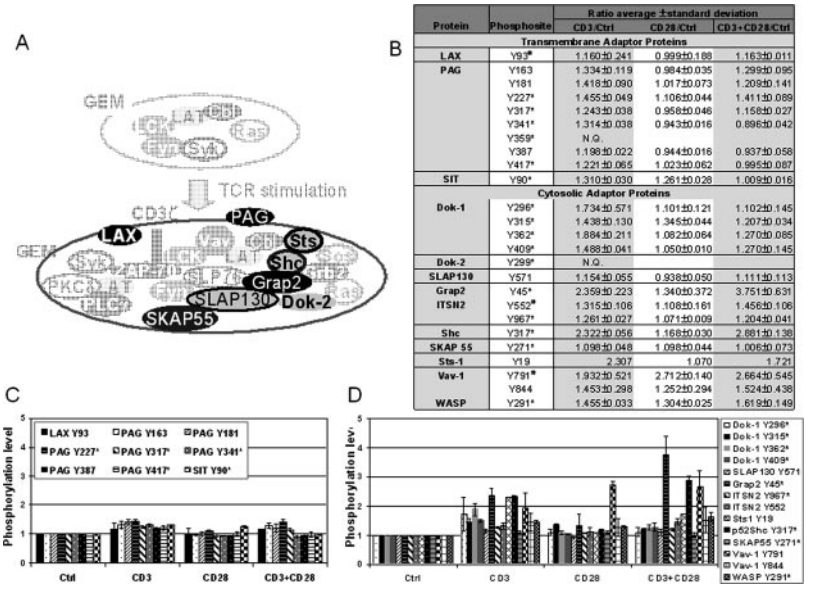

Protein	Phosphosite	Ratio average ±standard deviation		
		CD3/Ctrl	CD28/Ctrl	CD3+CD28/Ctrl
Transmembrane Adaptor Proteins				
LAX	Y93#	1.160±0.241	0.999±0.188	1.163±0.011
PAG	Y163	1.334±0.119	0.984±0.035	1.299±0.095
	Y181	1.418±0.090	1.017±0.073	1.209±0.141
	Y227*	1.455±0.049	1.106±0.044	1.411±0.089
	Y317*	1.243±0.038	0.958±0.046	1.158±0.027
	Y341*	1.314±0.038	0.943±0.016	0.896±0.042
	Y359#	N.Q.		
	Y387	1.198±0.022	0.944±0.016	0.937±0.058
	Y417*	1.221±0.065	1.023±0.062	0.995±0.087
SIT	Y90*	1.310±0.030	1.261±0.028	1.009±0.016
Cytosolic Adaptor Proteins				
Dok-1	Y296*	1.734±0.571	1.101±0.121	1.102±0.145
	Y315*	1.438±0.130	1.345±0.044	1.207±0.034
	Y362*	1.884±0.211	1.082±0.064	1.270±0.085
	Y409*	1.488±0.041	1.050±0.010	1.270±0.145
Dok-2	Y299*	N.Q.		
SLAP130	Y571	1.154±0.055	0.938±0.050	1.111±0.113
Grap2	Y45*	2.359±0.223	1.340±0.372	3.751±0.631
ITSN2	Y552#	1.315±0.106	1.108±0.161	1.456±0.106
	Y967*	1.261±0.027	1.071±0.009	1.204±0.041
Shc	Y317*	2.322±0.056	1.168±0.030	2.881±0.138
SKAP 55	Y271*	1.098±0.048	1.098±0.044	1.006±0.073
Sts-1	Y19	2.307	1.070	1.721
Vav-1	Y791*	1.932±0.521	2.712±0.140	2.664±0.545
	Y844	1.453±0.298	1.252±0.294	1.524±0.438
WASP	Y291*	1.455±0.033	1.304±0.025	1.619±0.149

FIGURE 5. Regulation of phosphorylation sites in adaptor proteins in response to T cell stimulation. *A,* Signaling proteins, including adaptor proteins, are recruited to GEM. LAX, lymphocyte transmembrane adaptor 1 or LAT-like membrane-associated protein; PAG; SIT, SHP2-interacting transmembrane adaptor protein; Dok-1;docking protein 1, downstream of tyrosine kinase 1; Fyb-120/130 or SLAP-130, Fyn-binding protein, SLP-76-associated protein 130; Grap2/Gads; ITSN2; Shc; SKAP-55, Src kinase-associated phosphoprotein of 55 kDa; Sts-1, Cbl-interacting protein Sts-1; and WASP. *B,* Quantification of specific tyrosine phosphorylation sites in both transmembrane and cytosolic adaptor proteins in response to CD3, CD28, and CD3/CD28 costimulation. Data represent mean of results obtained from two (#) or three experiments; ∗, Previously reported phosphorylation site. Phosphorylation of Sts-1 Tyr^{19} was detected in one analysis. N.Q., Nonquantified peptides due to the coelution of separate peptides with similar *m/z* values, resulting in mixed fragment ion spectrum and potential error in quantification. *C,* Changes in phosphorylation level of specific phosphorylation sites in transmembrane adaptor proteins in response to CD3, CD28, and CD3/CD28 costimulation. *D,* Changes in phosphorylation level of specific phosphorylation sites in cytosolic adaptor proteins in response to CD3 and/or CD28 stimulation. Ctrl, Control.

expression and protein phosphorylation profiles (12, 36). Interestingly, in the SOMs, Vav-1 Tyr^{791} is clustered together with both of the CD28 phosphorylation sites, as each of these sites displays greater phosphorylation following CD28 stimulation as compared with CD3 stimulation, and all are increased further under costimulation conditions. Another cluster implicated in the mechanism of costimulation response and common to both clustering methods features Vav-1 Tyr^{844}, calmodulin Tyr^{99}, and WASP Tyr^{291}. Overall, phosphorylation sites clustered together within the SOM are quite similar to those seen by hierarchical clustering (cf Fig. 4, *A* and *B*), providing additional validation to grouping of coregulated phosphorylation sites within these clusters.

Discussion

In this study, we present data quantifying the network level response to CD3/CD28 costimulation relative to CD3-stimulated, CD28-stimulated, and unstimulated Jurkat cells. By using a site-specific MS-based phosphoproteomics method, 87 phosphorylation sites could be quantified simultaneously across four cell states in triplicate experiments, enabling both the discovery of novel components and the monitoring of well-characterized signaling pathways. Information regarding phosphorylation of selected proteins is schematically encoded in Fig. 8*A* (CD3 stimulation response), *B* (CD28 stimulation response), and *C* (CD3/CD28 costimulation response). Stimulation of CD3 resulted in increased phosphorylation of CD3 ITAMs and upstream kinases such as Zap70 and PKC-δ to a level which was not further affected by CD3/CD28 costimulation (Fig. 8*A*). By comparison, CD28 stimulation resulted in a large increase in phosphorylation of CD28 and Vav-1 and smaller increases in phosphorylation levels of adaptor proteins such as Grap2, Dok-1, and WASP and kinases such as ERK1, ERK2, and PKC-δ (Fig. 8*B*). CD3/CD28 costimulation amplified tyrosine phosphorylation of CD28, MAPKs (p42 (ERK2), p44 (ERK1), p38), PLC-γ, and a few adaptor proteins (Grap2, Shc, and Vav-1) beyond levels detected following either CD3 or CD28 stimulation (Fig. 8*C* and Table I). These results indicate that the response to CD3/CD28 costimulation is largely due to the increase or decrease of phosphorylation levels on sites which are also utilized in response to CD3 stimulation, in agreement with the quantitative mechanism of T cell activation in response to CD3/CD28 costimulation. More specifically, data generated in this study suggest that the mechanism of costimulation to complete T cell activation may be enhanced tyrosine phosphorylation of PLC-γ/Shc/Grap2/Vav-1 leading to enhanced activation of downstream MAPKs and transactivation activities of AP-1 complex on IL-2 expression (1), which has been used as a marker for T cell activation in Jurkat cells for >20 years (35).

Interestingly, amplification of tyrosine phosphorylation in ERK1/2, p38, and Cdc2 by CD3/CD28 costimulation was the most noticeable change in this study and was accompanied by a decrease in threonine phosphorylation levels on the same peptides of these downstream components. Amplification of the singly (tyrosine) phosphorylated form might be explained simply by phosphatase activity leading to the conversion of the doubly (threonine and tyrosine) phosphorylated form back to the singly phosphorylated form. Among the known phosphatases affecting these proteins, we did not detect MAPK phosphatases or Cdc25C phosphatase, which specifically dephosphorylates Cdc2/cyclin B (37), potentially due to their regulation by serine phosphorylation while our study focused on tyrosine phosphorylation. Studies on MAPK phosphatases have focused on their specificity for individual MAPKs rather than specificity for either threonine or tyrosine (38).

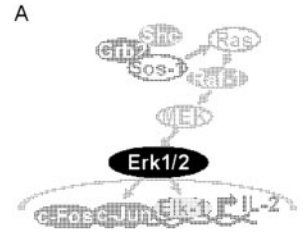

B

Protein	Phosphosite	Ratio average ± standard deviation		
		CD3/Ctrl	CD28/Ctrl	CD3+CD28/Ctrl
p42Erk2	T185* Y187*	9.517±1.657	1.193±0.070	6.476±0.623
	Y187*	5.781±0.340	1.175±0.118	10.496±0.824
p44Erk1	T202* Y204*	8.527±0.569	1.237±0.055	4.631±0.367
	Y204*	5.675±0.298	1.200±0.054	11.214±0.510
p38	Y182*	1.745±0.139	1.000±0.069	2.737±0.334

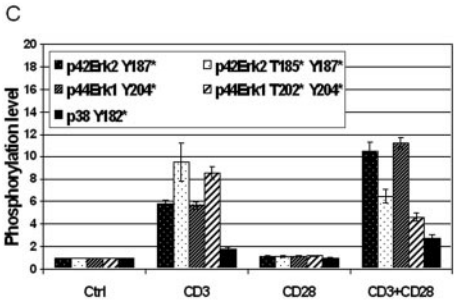

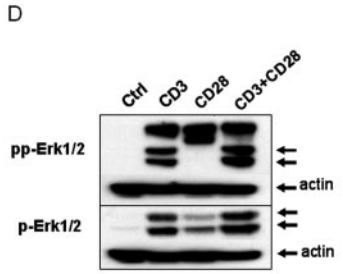

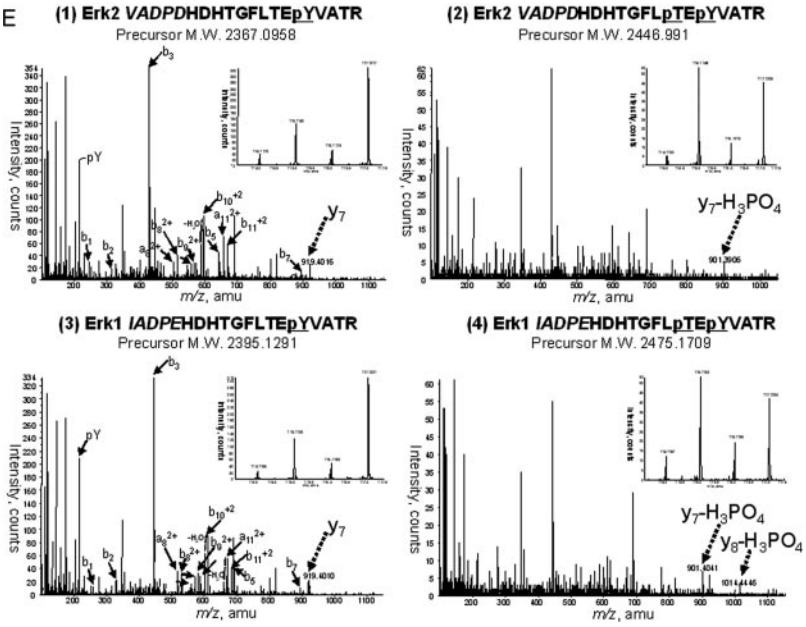

FIGURE 6. Regulation of phosphorylation sites in MAPKs in response to T cell stimulation. *A,* MAPK pathway. *B,* Quantification results of specific phosphorylation sites in MAPKs in response to CD3, CD28, and CD3/CD28 costimulation. Data represent mean of results obtained from three experiments; ∗, Previously reported phosphorylation site. *C,* Graphical representation of quantification data in *B*. *D,* Western blotting for specific phosphorylation sites in p44/42 MAPK using Abs recognizing either the doubly phosphorylated form of p44/42 (*upper blot*) or singly phosphorylated form of p44/42 (*lower blot*). Data are representative of three experiments. Actin was used as a loading control (Ctrl). *E,* Comparison of quantification of doubly and singly phosphorylated forms of both p42 ERK2 and p44 ERK1. MS/MS spectra for each peptide (graphs 1–4) contain y- and b-type ions which enable sequence and phosphorylation site assignment, while peak areas for iTRAQ marker ions enable quantification of phosphorylation from each sample. Solid arrows and molecular mass of each precursor peptide highlight evidence for the correct sequence while dashed arrows highlight evidence for the phospho-isoform of p42 ERK2 and p44 ERK1.

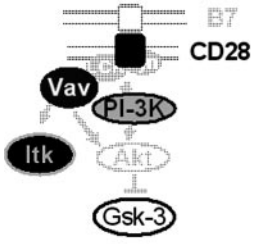

B

Protein	Phosphosite	Ratio average ± standard deviation		
		CD3/Ctrl	CD28/Ctrl	CD3+CD28/Ctrl
CD28	Y191*	1.885±0.053	3.545±0.402	4.726±0.627
	Y218*	3.097±0.403	3.784±0.550	4.658±0.387
PI-3K p85	Y467	1.163±0.083	1.042±0.033	0.982±0.028
Gsk-3	Y279*	1.060±0.051	1.048±0.060	0.967±0.094
Vav-1	Y791#*	1.932±0.521	2.712±0.140	2.664±0.545
	Y844	1.453±0.298	1.252±0.294	1.524±0.438
Itk/Tsk	Y512*	1.230±0.025	1.094±0.010	1.160±0.047

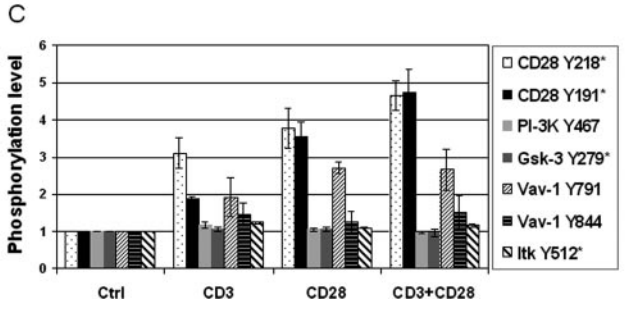

FIGURE 7. Regulation of phosphorylation sites in components of the CD28 signaling pathway in response to T cell stimulation. *A,* Components in CD28 signaling pathways: PI3K, Gsk3, and Itk. *B,* Quantification of specific tyrosine phosphosites in CD28, PI3K, Gsk3, Vav-1, and Itk in responses to CD3 and/or CD28 stimulation. Data represent mean of results obtained from two (#) or three experiments; ∗, Previously reported phosphorylation site. *C,* Graphical representation of quantification data in *B*. Ctrl, Control.

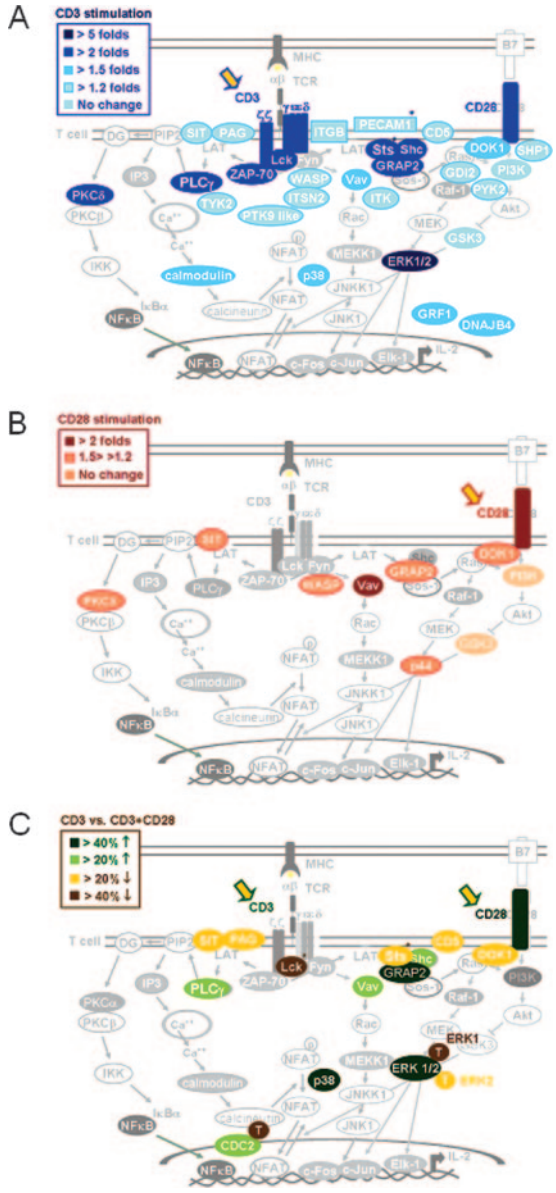

FIGURE 8. Regulation of phosphotyrosine protein networks in response to T cell stimulation. *A,* Response to CD3 stimulation. Fold increase in tyrosine phosphorylation of each protein was calculated by normalizing the CD3 stimulation-induced phosphorylation level against the control phosphorylation level. *B,* Response to CD28 stimulation. Fold increase in tyrosine phosphorylation of each protein was calculated by normalizing the CD28 stimulation-induced phosphorylation level against the control phosphorylation level. *C,* Effects of CD3/CD28 costimulation on tyrosine phosphorylation level in T cell signaling protein networks. Percent increase or decrease was calculated by (phosphorylation level in CD3/CD28 costimulation normalized against control)/(phosphorylation level in CD3 stimulation normalized against control) × 100 (%).

It is likely that activation of an alternate threonine-specific phosphatase could occur during CD3/CD28 costimulation, potentially delaying full activation of MAPKs while accelerating cell cycle entry by enhancing singly phosphorylated Cdc2 via decreased threonine phosphorylation. One outcome of T cell activation is cell cycle entry (39), and, at the G_2-M boundary, Cdc2 becomes dephosphorylated at both Thr^{14} and Tyr^{15}, resulting in entry into mitosis (40). Complementary information on phosphoserine/threonine protein networks and time-dependent phosphotyrosine activation may answer these questions, but network level quantification for low abundant phosphoserine/threonine proteins remains a challenging task due to the complexity and dynamic range of the serine/threonine phosphoproteome (41).

As suggested above, phosphatase activation may explain the decrease of doubly phosphorylated Cdc2 peptide (IGEGpTpYGVVYK) by 33.8% on costimulation and the increase of the singly phosphorylated peptide (IGEGTpYGVVYK) by 43.5%. However, it cannot adequately justify the results for ERK1 and ERK2, as the increase in tyrosine phosphorylation (97.6 and 81.6%, respectively) was much greater than could be accounted for the corresponding decrease in threonine phosphorylation (45.7 and 32%, respectively; Table I). Increased tyrosine phosphorylation of MAPKs after CD3/CD28 costimulation is therefore indicative of enhanced potentiation (potential future activation) of these proteins, a state that may be evident in analyses of later time points for these signaling networks. In sum, our study of CD3 and CD28 costimulation mechanism demonstrates an amplified phosphorylation level of upstream proteins such as CD28, PLC-γ, Shc, and Grap2, likely involvement of phosphatases in selected parts of the network, and enhanced tyrosine phosphorylation of MAPKs, suggesting an increase in network potentiation along with amplified signaling processes for complete T cell activation.

Along with identification of specific components and their interactions in signaling pathways, several efforts to understand the costimulatory mechanism in T cell signaling pathways at the systems level have recently started. For example, phosphorylation site-specific Ab-dependent protein microarray has been shown to be a sensitive tool to monitor alterations in phosphorylation levels of the known components in TCR signaling pathways (42). Compared with protein microarrays, our MS-based phosphoproteomics method combined with tyrosine peptide-specific immunoprecipitation (43) provides a complementary approach to understanding functional networks. Specifically, our method provides an Ab-independent tool for uncovering previously uncharacterized phosphorylation sites, as demonstrated by the identification of 43 previously uncharacterized tyrosine phosphorylation sites, 32 of which were quantified. Additionally, our MS-based method enables network level analysis while maintaining high-resolution quantitative information on phosphorylation site-specific regulation. For instance, by tandem MS it was possible to distinguish and quantify phosphorylation levels of singly and doubly phosphorylated ERK1 and ERK2 individually (Fig. 6*E*), while commercially available Abs cannot distinguish the two different MAPKs and appear to show cross-reactivity between singly and doubly phosphorylated forms of the kinase (Fig. 6*D*). It is also worth noting that sequence information from tandem MS was sufficient to distinguish and quantify phosphorylation at Tyr^{771} and Tyr^{775} in a peptide from PLC-γ, respectively (Fig. 3, *B* and *C*).

In this study, we have demonstrated a method enabling both identification and quantification of tyrosine-phosphorylated proteins at the network level from biologically relevant, TCR- and CD28-stimulated Jurkat cells. Several other groups have previously applied MS to investigate T cell signaling components. Rush et al. reported a list of tyrosine-phosphorylated proteins (43) and Tao et al. (44) adopted dendrimer chemistry to enrich phosphorylated peptides from pervanadate-treated Jurkat cells. Not surprisingly, pervanadate treatment dramatically enhances levels of protein tyrosine phosphorylation compared with anti-CD3 Ab treatment, which can be easily detected by anti-phosphotyrosine Western blotting (data not shown) and has been compared previously (45). Although pervanadate-stimulated cells can be useful, the strong activity of this compound and the lack of regulatory information in biological systems limit the utility of these cells to

development of methodology for improved identification of phosphoproteins. Other laboratories have used MS to investigate T cell signaling in response to particular stimuli; recently Salomon et al. (46) reported quantitative regulation of CD3-ζ in CD3/CD4-stimulated Jurkat cells using an external control and Zheng et al. reported a D_0/D_3-isotope-based quantitative methodology for IFN-α-treated Jurkat cells (47). Compared with these reports, we were able to scale down the number of cells 30- to 200-fold (from 0.3–2×10^9 to 1×10^7) per treatment and compare quantitative changes in more biologically relevant samples without an external control, thereby reducing errors associated with run-to-run variability. Isobaric-stable isotope tags (48) used in this method also provide several advantages, including coelution of the same peptide from all four different treatments and accumulation of MS signals in MS mode and MS/MS mode, resulting in higher sequence coverage and improved identification of low-abundant peptides.

Our site-specific quantitative phosphoproteomics approach identified networks of tyrosine-phosphorylated proteins triggered and regulated by CD3, CD28, and CD3/CD28 costimulation in Jurkat cells. Quantitative information suggests that CD3/CD28 costimulation may further activate the TCR signaling pathway mediated by enhanced phosphorylation of PLC-γ/Shc/Grap2/Vav-1 and their effects on downstream components including MAPKs. Although Vav-1 and WASP seem to be primarily activated in CD28 stimulation, potentially explaining a qualitative effect of costimulation leading to cytoskeletal rearrangement, enhanced phosphorylation of other upstream regulators suggests more quantitative than qualitative contribution by CD28 stimulation on CD3-stimulated TCR pathways. Application of bioinformatics tools to cluster coregulated phosphorylation events revealed and confirmed the presence of modules within tyrosine-phosphorylated signaling networks, such as the relationship between CD3 chains, tyrosine protein kinases, and adaptors. Our overall approach combining mass spectrometric analysis of tyrosine-phosphorylated peptides with clustering tools successfully identified, quantified, and delineated tyrosine-phosphorylated protein networks, highlighting at a network scale the systems' complexity in regulating response to stimulation and costimulation in T cells.

Acknowledgments

We thank D. Mathis and C. Benoist at the Joslin Diabetes Center and members of the White laboratory at Massachusetts Institute of Technology for helpful discussions.

Disclosures

The authors have no financial conflict of interest.

References

1. Germain, R. N., and I. Stefanova. 1999. The dynamics of T cell receptor signaling: complex orchestration and the key roles of tempo and cooperation. *Annu. Rev. Immunol.* 17: 467–522.
2. Cantrell, D. 1996. T cell antigen receptor signal transduction pathways. *Annu. Rev. Immunol.* 14: 259–274.
3. Samelson, L. E. 2002. Signal transduction mediated by the T cell antigen receptor: the role of adapter proteins. *Annu. Rev. Immunol.* 20: 371–394.
4. Kane, L. P., J. Lin, and A. Weiss. 2000. Signal transduction by the TCR for antigen. *Curr. Opin. Immunol.* 12: 242–249.
5. Lafferty, K. J., and A. J. Cunningham. 1975. A new analysis of allogeneic interactions. *Aust. J. Exp. Biol. Med. Sci.* 53: 27–42.
6. Acuto, O., and F. Michel. 2003. CD28-mediated co-stimulation: a quantitative support for TCR signalling. *Nat. Rev. Immunol.* 3: 939–951.
7. Rudd, C. E., and M. Raab. 2003. Independent CD28 signaling via VAV and SLP-76: a model for in *trans* costimulation. *Immunol. Rev.* 192: 32–41.
8. Michel, F., and O. Acuto. 2002. CD28 costimulation: a source of Vav-1 for TCR signaling with the help of SLP-76? *Sci. STKE* 2002: pe35.
9. Viola, A. 2001. The amplification of TCR signaling by dynamic membrane microdomains. *Trends Immunol.* 22: 322–327.
10. Dustin, M. L., and A. S. Shaw. 1999. Costimulation: building an immunological synapse. *Science* 283: 649–650.
11. Dustin, M. L., and J. A. Cooper. 2000. The immunological synapse and the actin cytoskeleton: molecular hardware for T cell signaling. *Nat. Immunol.* 1: 23–29.
12. Zhang, Y., A. Wolf-Yadlin, P. L. Ross, D. J. Pappin, J. Rush, D. A. Lauffenburger, and F. M. White. 2005. Time-resolved mass spectrometry of tyrosine phosphorylation sites in the epidermal growth factor receptor signaling network reveals dynamic modules. *Mol. Cell Proteomics* 4: 1240–1250.
13. Ficarro, S. B., M. L. McCleland, P. T. Stukenberg, D. J. Burke, M. M. Ross, J. Shabanowitz, D. F. Hunt, and F. M. White. 2002. Phosphoproteome analysis by mass spectrometry and its application to *Saccharomyces cerevisiae*. *Nat. Biotechnol.* 20: 301–305.
14. Watts, J. D., M. Affolter, D. L. Krebs, R. L. Wange, L. E. Samelson, and R. Aebersold. 1994. Identification by electrospray ionization mass spectrometry of the sites of tyrosine phosphorylation induced in activated Jurkat T cells on the protein tyrosine kinase ZAP-70. *J. Biol. Chem.* 269: 29520–29529.
15. Kong, G., M. Dalton, J. B. Wardenburg, D. Straus, T. Kurosaki, and A. C. Chan. 1996. Distinct tyrosine phosphorylation sites in ZAP-70 mediate activation and negative regulation of antigen receptor function. *Mol. Cell. Biol.* 16: 5026–5035.
16. Parekh, D. B., W. Ziegler, and P. J. Parker. 2000. Multiple pathways control protein kinase C phosphorylation. *EMBO J.* 19: 496–503.
17. Brodie, C., and P. M. Blumberg. 2003. Regulation of cell apoptosis by protein kinase cδ. *Apoptosis* 8: 19–27.
18. Wang, Q., X. Wang, and B. M. Evers. 2003. Induction of cIAP-2 in human colon cancer cells through PKCδ/NF-κB. *J. Biol. Chem.* 278: 51091–51099.
19. Uddin, S., A. Sassano, D. K. Deb, A. Verma, B. Majchrzak, A. Rahman, A. B. Malik, E. N. Fish, and L. C. Platanias. 2002. Protein kinase C-δ (PKC-δ) is activated by type I interferons and mediates phosphorylation of Stat1 on serine 727. *J. Biol. Chem.* 277: 14408–14416.
20. Clements, J. L., N. J. Boerth, J. R. Lee, and G. A. Koretzky. 1999. Integration of T cell receptor-dependent signaling pathways by adapter proteins. *Annu. Rev. Immunol.* 17: 89–108.
21. Liu, S. K., and C. J. McGlade. 1998. Gads is a novel SH2 and SH3 domain-containing adaptor protein that binds to tyrosine-phosphorylated Shc. *Oncogene* 17: 3073–3082.
22. Walk, S. F., M. E. March, and K. S. Ravichandran. 1998. Roles of Lck, Syk and ZAP-70 tyrosine kinases in TCR-mediated phosphorylation of the adapter protein Shc. *Eur. J. Immunol.* 28: 2265–2275.
23. Ravichandran, K. S., K. K. Lee, Z. Songyang, L. C. Cantley, P. Burn, and S. J. Burakoff. 1993. Interaction of Shc with the ζ chain of the T cell receptor upon T cell activation. *Science* 262: 902–905.
24. Cory, G. O., R. Garg, R. Cramer, and A. J. Ridley. 2002. Phosphorylation of tyrosine 291 enhances the ability of WASp to stimulate actin polymerization and filopodium formation: Wiskott-Aldrich Syndrome protein. *J. Biol. Chem.* 277: 45115–45121.
25. Torres, E., and M. K. Rosen. 2003. Contingent phosphorylation/dephosphorylation provides a mechanism of molecular memory in WASP. *Mol. Cell* 11: 1215–1227.
26. McGavin, M. K., K. Badour, L. A. Hardy, T. J. Kubiseski, J. Zhang, and K. A. Siminovitch. 2001. The intersectin 2 adaptor links Wiskott-Aldrich syndrome protein (WASp)-mediated actin polymerization to T cell antigen receptor endocytosis. *J. Exp. Med.* 194: 1777–1787.
27. Carpino, N., D. Wisniewski, A. Strife, D. Marshak, R. Kobayashi, B. Stillman, and B. Clarkson. 1997. $p62^{dok}$: a constitutively tyrosine-phosphorylated, GAP-associated protein in chronic myelogenous leukemia progenitor cells. *Cell* 88: 197–204.
28. Brdicka, T., D. Pavlistova, A. Leo, E. Bruyns, V. Korinek, P. Angelisova, J. Scherer, A. Shevchenko, I. Hilgert, J. Cerny, et al. 2000. Phosphoprotein associated with glycosphingolipid-enriched microdomains (PAG), a novel ubiquitously expressed transmembrane adaptor protein, binds the protein tyrosine kinase csk and is involved in regulation of T cell activation. *J. Exp. Med.* 191: 1591–1604.
29. Cook, J. A., A. August, and A. J. Henderson. 2002. Recruitment of phosphatidylinositol 3-kinase to CD28 inhibits HIV transcription by a Tat-dependent mechanism. *J. Immunol.* 169: 254–260.
30. Cook, J. A., L. Albacker, A. August, and A. J. Henderson. 2003. CD28-dependent HIV-1 transcription is associated with Vav, Rac, and NF-κB activation. *J. Biol. Chem.* 278: 35812–35818.
31. Teng, J. M., P. D. King, A. Sadra, X. Liu, A. Han, A. Selvakumar, A. August, and B. Dupont. 1996. Phosphorylation of each of the distal three tyrosines of the CD28 cytoplasmic tail is required for CD28-induced T cell IL-2 secretion. *Tissue Antigens* 48: 255–264.
32. Heyeck, S. D., H. M. Wilcox, S. C. Bunnell, and L. J. Berg. 1997. Lck phosphorylates the activation loop tyrosine of the Itk kinase domain and activates Itk kinase activity. *J. Biol. Chem.* 272: 25401–25408.
33. Astoul, E., C. Edmunds, D. A. Cantrell, and S. G. Ward. 2001. PI 3-K and T-cell activation: limitations of T-leukemic cell lines as signaling models. *Trends Immunol.* 22: 490–496.
34. Shan, X., M. J. Czar, S. C. Bunnell, P. Liu, Y. Liu, P. L. Schwartzberg, and R. L. Wange. 2000. Deficiency of PTEN in Jurkat T cells causes constitutive localization of Itk to the plasma membrane and hyperresponsiveness to CD3 stimulation. *Mol. Cell. Biol.* 20: 6945–6957.
35. Abraham, R. T., and A. Weiss. 2004. Jurkat T cells and development of the T-cell receptor signalling paradigm. *Nat. Rev. Immunol.* 4: 301–308.
36. Tamayo, P., D. Slonim, J. Mesirov, Q. Zhu, S. Kitareewan, E. Dmitrovsky, E. S. Lander, and T. R. Golub. 1999. Interpreting patterns of gene expression with

self-organizing maps: methods and application to hematopoietic differentiation. *Proc. Natl. Acad. Sci. USA* 96: 2907–2912.
37. Roshak, A. K., E. A. Capper, C. Imburgia, J. Fornwald, G. Scott, and L. A. Marshall. 2000. The human polo-like kinase, PLK, regulates cdc2/cyclin B through phosphorylation and activation of the cdc25C phosphatase. *Cell Signal* 12: 405–411.
38. Chu, Y., P. A. Solski, R. Khosravi-Far, C. J. Der, and K. Kelly. 1996. The mitogen-activated protein kinase phosphatases PAC1, MKP-1, and MKP-2 have unique substrate specificities and reduced activity in vivo toward the ERK2 sevenmaker mutation. *J. Biol. Chem.* 271: 6497–6501.
39. Bauer, B., and G. Baier. 2002. Protein kinase C and AKT/protein kinase B in $CD4^+$ T-lymphocytes: new partners in TCR/CD28 signal integration. *Mol. Immunol.* 38: 1087–1099.
40. Riabowol, K., G. Draetta, L. Brizuela, D. Vandre, and D. Beach. 1989. The cdc2 kinase is a nuclear protein that is essential for mitosis in mammalian cells. *Cell* 57: 393–401.
41. Beausoleil, S. A., M. Jedrychowski, D. Schwartz, J. E. Elias, J. Villen, J. Li, M. A. Cohn, L. C. Cantley, and S. P. Gygi. 2004. Large-scale characterization of HeLa cell nuclear phosphoproteins. *Proc. Natl. Acad. Sci. USA* 101: 12130–12135.
42. Chan, S. M., J. Ermann, L. Su, C. G. Fathman, and P. J. Utz. 2004. Protein microarrays for multiplex analysis of signal transduction pathways. *Nat. Med.* 10: 1390–1396.
43. Rush, J., A. Moritz, K. A. Lee, A. Guo, V. L. Goss, E. J. Spek, H. Zhang, X. M. Zha, R. D. Polakiewicz, and M. J. Comb. 2005. Immunoaffinity profiling of tyrosine phosphorylation in cancer cells. *Nat. Biotechnol.* 23: 94–101.
44. Tao, W. A., B. Wollscheid, R. O'Brien, J. K. Eng, X.-J. Li, B. Bodenmiller, J. D. Watts, L. Hood, and R. Aebersold. 2005. Quantitative phosphoproteome analysis using a dendrimer conjugation chemistry and tandem mass spectrometry. *Nat. Methods* 2: 591–598.
45. Secrist, J. P., L. A. Burns, L. Karnitz, G. A. Koretzky, and R. T. Abraham. 1993. Stimulatory effects of the protein tyrosine phosphatase inhibitor, pervanadate, on T-cell activation events. *J. Biol. Chem.* 268: 5886–5893.
46. Salomon, A. R., S. B. Ficarro, L. M. Brill, A. Brinker, Q. T. Phung, C. Ericson, K. Sauer, A. Brock, D. M. Horn, P. G. Schultz, and E. C. Peters. 2003. Profiling of tyrosine phosphorylation pathways in human cells using mass spectrometry. *Proc. Natl. Acad. Sci. USA* 100: 443–448.
47. Zheng, H., P. Hu, D. F. Quinn, and Y. K. Wang. 2005. Phosphotyrosine proteomic study of interferon α signaling pathway using a combination of immunoprecipitation and immobilized metal affinity chromatography. *Mol. Cell Proteomics* 4: 721–730.
48. Ross, P. L., Y. N. Huang, J. N. Marchese, B. Williamson, K. Parker, S. Hattan, N. Khainovski, S. Pillai, S. Dey, S. Daniels, et al. 2004. Multiplexed protein quantitation in *Saccharomyces cerevisiae* using amine-reactive isobaric tagging reagents. *Mol. Cell Proteomics* 3: 1154–1169.